Fluorescent aptasensor for ofloxacin detection based on the aggregation of gold nanoparticles and its effect on quenching the fluorescence of Rhodamine B

Zhiyu Yan, Haoyang Yi, Lumei Wang, Xiaotong Zhou, Rui Yan, Dongwei Zhang, Song Wang, Lantian Su, Shanshan Zhou

PII:	S1386-1425(19)30593-1
DOI:	https://doi.org/10.1016/j.saa.2019.117203
Article Number:	117203
Reference:	SAA 117203
To appear in:	*Spectrochimica Acta Part A: Molecular and Biomolecular Spectroscopy*
Received date:	30 March 2019
Revised date:	26 May 2019
Accepted date:	26 May 2019

Please cite this article as: Z. Yan, H. Yi, L. Wang, et al., Fluorescent aptasensor for ofloxacin detection based on the aggregation of gold nanoparticles and its effect on quenching the fluorescence of Rhodamine B, Spectrochimica Acta Part A: Molecular and Biomolecular Spectroscopy, https://doi.org/10.1016/j.saa.2019.117203

Fluorescent aptasensor for ofloxacin detection based on the aggregation of gold nanoparticles and its effect on quenching the fluorscence of Rhodamine B

Zhiyu Yan[a, #] · Haoyang Yi[a, #] · Lumei Wang[a, *] · Xiaotong Zhou[a] · Rui Yan[b] · Dongwei Zhang[a] · Song Wang[a] · Lantian Su[a] · Shanshan Zhou[c]

[a] *School of Agriculture and Biology, Key Laboratory of Urban Agriculture, Ministry of Agriculture, Bor S. Luh Food Safety Research Center, Shanghai Jiao Tong University, Shanghai, 200240, PR China*

[b] *Meteorological Bureau of Liupanshui, Liupanshui 553000, PR China*

[c] *College of Environment, Zhejiang University of Technology, Hangzhou 310014, PR China*

[#] *These author contributed equally to this work and should be considered co-first authors*

* *Corresponding author, E-mail: zjuwlm@163.com; Tel: +86-21-34206924; Fax: +86-21-34205762.*

Abstract:

This paper proposes the idea of building a fluorescent biosensor for ofloxacin (OFL) determination in aqueous and milk samples by label–free OFL–specific aptamer, gold nanoparticles (AuNPs) and Rhodamine B (RB). In the absence of OFL, AuNPs are coated with OFL aptamer and maintain dispersed in the high concentration of NaCl. The dispersed AuNPs could reduce the strong fluorescence intensity of RB efficiently. By contrast, in the presence of OFL, OFL is combined with aptamer to form stable compounds, causing the aptamers separated from the surface of AuNPs, thus AuNPs would be exposed in the solution. And the aggregated AuNPs will not quench the fluorescence intensity of RB. Through the distinction of the fluorescence intensity, the concentration of OFL could be detected in aqueous and milk samples quantitatively. The convenient and specific fluorescent assay for OFL is established with a linear range (R =0.9907) from 20 to 300 nM and a detection limit of 1.66 nM in aqueous solution, and a linear range (R =0.9963) from 20 to 300 nM and a detection limit of 4.61 nM (1.66 μg/L) in milk samples. With the good sensitivity and selectivity, this biosensor has good application potential to detect OFL in food and environmental samples.

Key words:

AuNPs · Rhodamine B · Aptamer · Ofloxacin · Milk · Assay

1. Introduction

Ofloxacin (OFL) is a representative and wide-used synthetic fluoroquinolone antibiotic, which has excellent broad-spectrum activity against gram-negative and gram-positive bacteria by interfering enzyme DNA gyrase for the synthesis of bacterial DNA [1-3]. However, extensive use of OFL in human and veterinary medicines cause incompletely metabolism in bodies [4,5] and degradation-resistant and high absorption properties to accumulate in the environment, especially the soil. And it could not only pollute the aquatic environment even at low concentrations, but also causes toxic effects on surface water and surface water [6-8]. Hence, OFL is considered as a high potential pollutant, which has raised various environmental issues and the emergence of bacterial resistance until now [9]. Besides, by contrast with other typical fluoroquinolone like ciprofloxacin, although ciprofloxacin is widely used in medical treatment, studies have found that the concentration of ofloxacin in Italian hospital sewage exceeds that of ciprofloxacin, and the annual consumption of ofloxacin exceeds ciprofloxacin 1000 times [6] as well as since 2014, ofloxacin has gradually replaced the fourth-generation gatifloxacin and moxifloxacin, which were originally used in large quantities, and it is dominant in the use of quinolones [10]. And it is demonstrated that OFL can induce morphologic fibril formation of lysozyme, indicates that caution should be exercised in the environmental contact of OFL in patients susceptible to various aggregation diseases [11].

Many countries have issued standards for the concentrations of OFL in aquatic and animal products [12]. Therefore, it is necessary and significant to develop valid and quick methods for the detection of OFL in the environment and food samples.

Traditional methods have been used in the quantification detection of OFL in aquatic or milk samples such as high-performance liquid chromatography (HPLC) [13,14], electrochemical methods [15-17], fluorescence detection [18], extraction spectrophotometric method [19] and liquid chromatograph mass spectrometer (LC-MS) [20,21]. Although they have high sensitivity and good selectivity, expensive instruments, professional operators, complex pretreatments, and time-consuming process have restricted the applications for the detection of OFL in waste-water field or food test.

Since the vitro selection technique named SELEX (Systematic Evolution of Ligands by Exponential Enrichment) reported in 1990 [22,23], aptamers have been developed as recognition elements in many biosensors due to the good selectivity, high specificity, flexible modification and high stability [24,25]. The OFL-specific aptamer [26], which was selected in 2015, has high affinity to detect OFL with relative average deviation (R_D) of 0.11(± 0.06) nM. and it has been used to detect OFL by thiolated aptamer-based electrochemical methods which shows good selectivity, but LOD is limited at 1 nM and needs complex preprocessing [27]. In 2018, unmodified colorimetric methods using gold nanoparticles (AuNPs) were established [28]. The method shows advantages like observable, convenient and cheap, but its LOD based on colorimetric method still has potential to optimize to meet the need of more accurate analysis and its practical application is limited to simple samples such as tap water, artificial urine.

AuNPs has shown controlled geometrical, optical, and surface chemical properties [29], which lead to its participation in various optical determinations of small organic molecules, metal ions and proteins [30,31] when the target is not present, the aptamer can be coated on the surface of AuNPs to prevent the trend of aggregation after adding NaCl into the solution, while if there are

targets, AuNPs will be aggregated under the action of NaCl, since the specific reaction between target with aptamer. Therefore, the remarkably different absorbance between being dispersed and aggregated could been utilized extensively in aptasensor for quantitative analysis. Besides, the dispersed AuNPs can quench photoluminescence effects on some fluorescence matters [32] based on fluorescence resonance energy transfer (FRET) [33]. And FRET is a nonradiative energy transfer interaction between two electronic excited states of fluorescent substances wherein energy is transferred from RB as an excited fluorophore in a non-photonmediated manner to a colored acceptor like AuNPs depending primarily on the donor-acceptor distance, relative orientation, and wavelength match between the donor's emission and the acceptor's absorbance, which means that the fluorescence of RB can be quenched quantitatively by AuNPs under different degree of aggregation. Additionally, Rhodamine B (RB) is a well-known dye with strong fluorescence and high solubility [34], which can be used for the fluorescent determination.

Thus, dispersed AuNPs have ability to greatly quench the fluorescence of RB while aggregated AuNPs show a weaker quenching ability, causing the difference in fluorescence intensity by the aggregation degree of AuNPs.

The effective and accurate detection of antibiotics in actual milk or other foods using sensing system based on aptamer has been concerned as a promising and practical research field [35]. In the study, a sensitive, simple fluorescent quantitative detection for OFL was established on the basis of OFL-specific aptamer, AuNPs and RB. The method is based on NaCl–induced colorimetric aptamer-based detection [28,29] and RB is used as a signal amplifier [32] to detect the OFL in aqueous and milk samples.

2. **Materials & Methods**

2.1 Reagents and chemicals

The sequence of OFL–specific aptamer is 5’ –ATACCAGCTTATTCAATTGCAGGGTATCTGAGGCTTGATCTACTAAATGTCGTGGGGCATTGCTATTGGCGTTGATACGTACAATCGTAATCAGTTAG–3’(98–mer) [26], which is different with aptamers used in the previous study, mainly reflected in the sequences and thiolated modification(5’-SH-(CH2)6-ATACCAGCTTATTCAATTAGTTGTGTATTGAGGTTTGATCTAGGCATAGTCAACAGAGCACGATCGATCTGGCTTGTTCTACAATCGTAATCAGTTAG-3’) [27]. This label-free aptamer was synthesized by Sangon Biotechnology Inc. (Shanghai, China, www.sangon.com). The centrifuge tube with the aptamer powder was centrifuged the speed of 12000 r for one minute to gather the aptamer in the bottom, and then the aptamer was dissolved in ultra-pure water at 100 μM and stored at 4 °C. RB, ofloxacin (OFL), ampicillin (AMP), tetracycline (TET), kanamycin (KAN), thiamphenicol (TAP), enrofloxacin (ENR), 7–aminocephalosporanic acid (7–ACA) were obtained from Aladdin Biotechnology Inc (Shanghai, China). Nalidixic acid (NAD) and carbendazim (CBZ) were bought from Sigma–Aldrich (St. Louis, MO, USA; www.sigmaaldrich.com). Ciprofloxacin (CIP) and lomefloxacin hydrochloride （LOM) were gained from Shanghai Mokai Biotechnology Co., Ltd. (Shanghai, China). Enoxacin (ENO) was gotten from Shanghai Gaoxinhua Glass Instrument Inc. (Shanghai, China). Pefloxacin (PEF) was bought from Qiaoyi Biotechnology CO., Ltd. (Shanghai, China). Sodium chloride (NaCl) and trisodium citrate ($C_6H_5Na_3O_7$) were bought from Beijing Chemical Reagents

Company (Beijing, China). $HAuCl_4 \cdot 4H_2O$ and 3–(N–morpholino) propanesulfonic acid (MOPS, 10 mM) were purchased from Sinopharm Chemical Reagent Co., Ltd. (Shanghai, China, en.reagent.com.cn). The pH of MOPS was pretreated with sodium hydroxide (NaOH) and hydrochloric acid (HCl) to 3, 4, 5, 6, 7, 8, 9, 10. Ultrapure water was purified by Milli-Q plus Advantage A10 System (Milli-Q plus, Millipore Inc., Bedford, MA, USA) for use. Milk samples with the fat content of 3.1%, protein content of 2.9% were purchased from local market (Shanghai, China).

2.2 Instrumentations

F-4500 fluorescence spectrophotometer (Hitachi, Japan) was used to measure the fluorescence intensity. The Infinite M200 Pro microplate spectrophotometer (Tecan Austria GmbH, Salzburg, Austria) was employed to measure the absorbance value of the solutions, and the 96-well microplates were purchased from Thermo Fisher Scientific Inc. (Nunclon, Denmark). Thermostatic incubating device (Eppendorf, China) was used to maintain the incubating temperatures at 25 °C. Circular dichroism spectroscopy (CD; J–815, Jasco, Japan) was utilized to characterize the conformational changes of OFL aptamer. Transmission electron microscope (TEM) (JEM2010HT, Hitachi, Japan) was used to determine the morphology of AuNPs in different conditions. Dynamic light scattering (DLS) (Zetasizer Nano S; Malvern, England) was used to measure the average diameter of AuNPs.

2.3 Preparation and characterization of AuNPs

AuNPs were prepared by sodium citrate reduction of $HAuCl_4$ solution [36]. First, all the glassware used in the experiment were cleaned by freshly prepared 1:3 (v/v) HNO_3/ HCl and rinsed in ultrapure water thoroughly and dried in air. Then, 10.5 mL of 1% (w/v) trisodium citrate solution was added quickly to the boiling solution of $HAuCl_4 \cdot 4H_2O$ (100 mL, 0.03%, w/w) and stirred for 30 min to synthesize AuNPs. After the color of boiling solution gradually changed from grey, blue, deep purple to wine red, the solution was stopped heating and stirred for 20 min. Finally, the resulting solution was cooled sufficiently and filtered with 0.22 μm ultrafiltration membranes, and then stored in dark glass bottle at 4 °C for further use.

2.4 Interactions among AuNPs, OFL, aptamer, and NaCl

TThe CD spectrum of two samples was measured to characterize the interaction between OFL and the aptamer: (a) 200 nM aptamer; (b) 200 nM aptemer + 2 μM OFL. Sample (a) was measured directly and sample (b) was measured after a 30–min incubation. The volume of each system was 500 μL.

The dynamic light scattering (DLS) was used to test the average diameter of AuNPs by Zetasizer Nano S in four different circumstances: (a) AuNPs; (b) AuNPs + 10 nM aptamer + 120 mM NaCl; (c) AuNPs + 10 nM aptamer + 120 mM NaCl + 500 nM OFL; (d) AuNPs + 10 nM aptamer + 120 mM NaCl + 1000 nM OFL. The volume of each sample was set to 5 mL. Sample (a) was tested directly. Sample (b) was tested after two steps that was a 30–min incubation between aptamer and AuNPs, following a 10–min reaction after adding NaCl. In sample (c) and sample (d),

the aptamers and OFL were incubated for 30 min firstly, following a 30–min incubation with AuNPs. Then the NaCl solution was added for a 10-min incubation. At last, the particle size of AuNPs was measured. Meanwhile, each sample of 500 μL was tested by transmission electron microscope (TEM) to obtain the morphological changes of AuNPs.

2.5 Measurement of absorbance and fluorescence

Each experiment system was set as 500 μL, containing 100 μL AuNPs. The initial concentration of aptamer, NaCl, and OFL were 500 nM, 2 M and 100 mM. The original experimental temperature was 25 °C, and the initial pH of MOPS was 7. Each experiment was repeated for at least three times.

Before adding RB to the sensing system, the absorbances at 520 nm (A520) and 650 nm (A650) were recorded to represent the relative content of dispersed and aggregated AuNPs. Thus, the value A = A650/A520 was represented the aggregation degree of AuNPs. To eliminate the influence of experimental instrument errors and build mathematical model, the value ΔA ($\Delta A = A–A_0$) was calculated to reflect the difference of samples in aggregation degree of AuNPs between the sample solutions with OFL (A) and the blank solutions without OFL (A_0). Besides, the value ΔA was also utilized to optimize experimental conditions before adding RB.

When adding RB to the sensing system, sensitive fluorescence intensities of the sample and the blank solutions (F, F_0) were measured by F-4500 fluorescence spectrophotometer with the excitation slit width of 10 nm, the emission slit width of 2.5 nm, photomultiplier voltage of 700 V and the excitation wavelength at 520 nm. Hence, the correctional value ΔF ($\Delta F = F–F_0$) was calculated to estimate the concentration of OFL.

2.6 Optimization of experimental conditions

The optimization of the concentration of NaCl and aptamer, the temperature and the pH of the MOPS buffer were performed. When the NaCl concentration was optimized through colorimetric procedure, 100 μL AuNPs in the sensing system was treated with increasing concentration of NaCl (0, 20, 40, 60, 80, 100, 120, 140, 160 mM) in 1.5mL centrifugation tubes with MOPS buffer (400, 395, 390, 385, 380, 370, 365, 360 μL, 10 mM, pH=7) and the total volume eventually reached to 500 μL. After a 10–min incubation in 25 °C, the absorbance value A520 and A650 was measured. The value A=A650/A520 was calculated, which could reach the maximum value when AuNPs was completely aggregated by the NaCl solution. The minimum concentration of NaCl that fully aggregated AuNPs was chosen as the optimal concentration.

The aptamer with different concentration (0, 2, 4, 6, 8, 10, 12, 14, 16 nM) was added to the sample system contained MOPS buffer and 1 μM OFL, and OFL was replaced by the same volume of MOPS buffer in the blank system. All the experimental systems were incubated for 20 min, then adding 100 μL AuNPs, and the solution was incubated for another 20 min to fully combine aptamer and AuNPs. Finally, the optimized volume of NaCl was added, and after incubating for 10 min, the value ΔA ($\Delta A=A–A_0$) was obtained. The concentration which led to the maximum value of ΔA was chosen as the optimal aptamer concentration.

To optimize the incubating temperature, the temperature of thermostatic incubating device was set as 15, 20, 25, 30, 35, 40, 45, 50 ℃. To optimize the pH of the buffer, MOPS with different

pH (3, 4, 5, 6, 7, 8, 9, 10) were used. The process was the same as the optimization of aptamer on the basis of the optimized concentration of aptamer, and the value ΔA ($\Delta A=A-A_0$) were obtained by monitoring the change of absorbance. The temperature and the pH that led to the highest ΔA were chosen in each optimizing test.

The concentration of RB was optimized by fluorescent method. Firstly, 1 μM OFL, MOPS buffer and the optimized concentration of aptamer were added into the system. After incubating for 20 min, 100 μL AuNPs was added and the system was incubated for 20 min, and then the optimized concentration of NaCl was added before another 10–min incubation. Afterwards, different concentrations of RB (2, 4, 6, 8, 10, 12, 14 μM) were added to incubate between dispersed AuNPs and RB for 10 min. Finally, the fluorescence intensity (F) of the solution was measured, and the value ΔF ($\Delta F=F-F_0$) was obtained. The concentration which led to the maximum value of ΔF was chosen as the optimal concentration.

2.7 Sensitivity and selectivity of the detecting system

To evaluate the responsivity of the fluorescence aptasensor and exclude possibility of false positive results, sensitivity and selectivity of the sensing system were tested. Firstly, 10 μL aptamer and different concentration of OFL (0, 20, 40, 80, 120, 160, 200, 300, 400, 500, 600, 700, 800, 1000, 1500 nM) were incubated with MOPS buffer for 20 min. And then, adding 100 μL AuNPs for another 20-min incubation. Afterwards, the optimized concentration of NaCl was added before another 10-min incubation. At last, adding 9 μM RB for 10 mins to calculate the fluorescence intensity (ΔF), which was used to investigate the sensitivity.

Selectivity test carried out control experiments using several antibiotics, such as AMP, TET, KAN, 7-ACA, TAP, ENO, structure analogues of OFL like ENR, NAD, CIP, PEF and LOM, pesticide like CBZ and metal ion Cd^{2+} of 1 μM instead of OFL in optimized conditions. The value ΔF of OFL and other interfering substances were calculated.

2.8 Application in milk samples

Firstly, the milk protein precipitator was prepared by mixing 12 mL of methanol and 2 mL of 85% phosphoric acid. The solution was added into 5 mL milk in a 20 mL centrifuge tube, which was oscillated for 5 min and stored in a refrigerator at 4 °C for 2 hours under the following process. After the centrifugation at 5000 r for 5 min, the solution with precipitated lactoprotein was filtered with 0.22 μm filter membrane, and eventually the clarified liquid was saved in the centrifuge tube for further use.

The milk sample was used to dissolve OFL in place of MOPS buffer in the sensing system, and another sensitivity study with OFL dissolved in milk was carried out. As a result, the working curve of fluorescence aptasensor in milk samples and the limit of detection (LOD) were founded. The stability of the sensing system in milk samples was evaluated by comparing the working curve with the former testing curve, and contrasting LOD with the maximum residue level (MRL) of OFL in food security standard.

To check the accuracy of aforementioned sensitivity test in milk samples, several milk samples were spiked OFL to 0, 50, 100, 150 and 200 nM for test by the established aptasensor. The recovery rate and relative standard deviation (RSD) of the samples were calculated.

3. Results and discussion

3.1 Principle of the fluorescent aptasensor

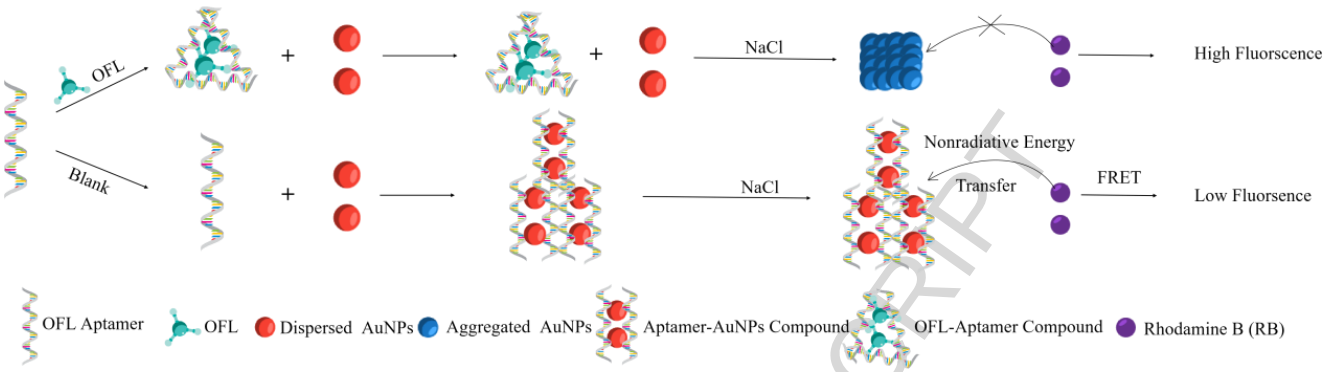

Scheme. 1 Schematic diagram of the fluorescent assay for OFL detection based on aggregated AuNPs quenching the original fluorescence of Rhodamine B in NaCl solution.

The sensing principle of this aptasensor based on fluorescence is showed in Scheme 1. At the beginning of the experiment, when target (OFL) exists in the solution, OFL could bind with OFL aptamer due to the strong affinity to form OFL-aptamer compounds, and the specific binding effects between them are more stable than the interaction between DNA and AuNPs based on Vander Waals, thus AuNPs are aggregated by the high concentration of NaCl due to the charge effect between the negative charge of AuNPs and the positive charge of NaCl. And the aggregated AuNPs reduce the ability to quench the fluorescence of RB. When OFL are absent in the solution, the surface of AuNPs are coated with the OFL aptamers through the interaction under Vander Waals, leading to the AuNPs–Aptamer compound, which could protect AuNPs from aggregating even though in the high concentration of NaCl. Besides, the dispersed AuNPs are able to quench the high fluorescence of RB well cause of FRET. Therefore, the fluorescent intensity fluctuation of RB based on the quenching ability of dispersed and aggregated AuNPs can be an amplified signal to detect the concentration of OFL in the solution quantitatively.

3.2 Characterization of AuNPs and aptamer

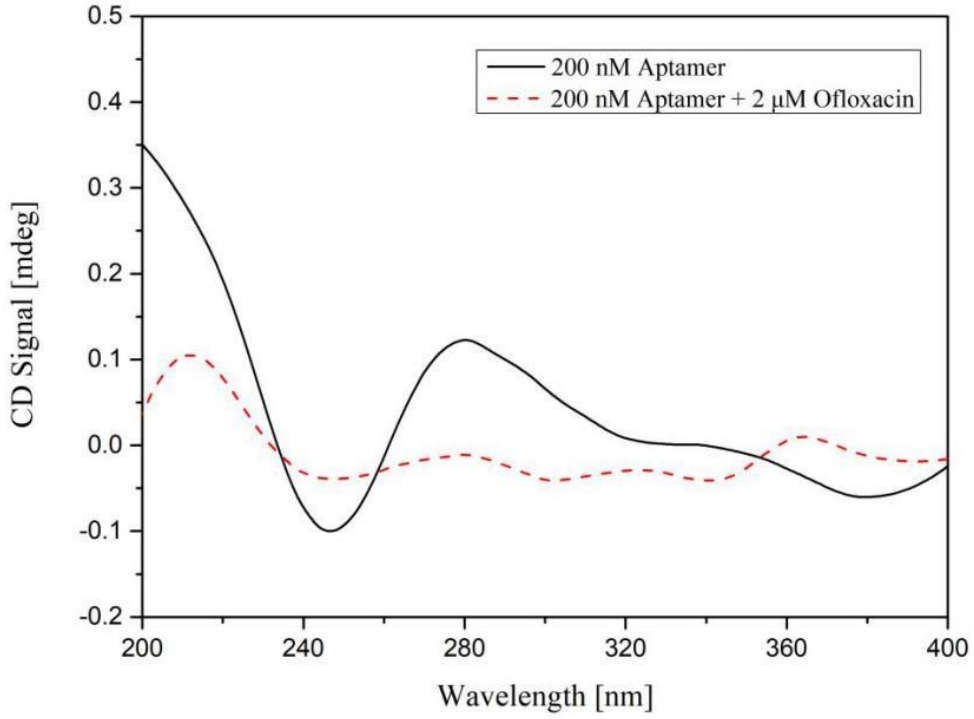

Fig. 1 Circular dichrosim (CD) spectra of aptamer treated with OFL in different condition:(a) 200 nM aptamer; (b) 200 nM aptamer + 2 μM OFL.

CD spectrum is operative to illustrate the conformational changes of oligonucleotides or DNA. Hence, the aptamer conformation changes due to the interaction between aptamer and OFL in the system could be obtained by the change of CD spectrum. Fig. 1 shows that the OFL aptamer has a negative peak at 240–260 nm and a positive peak at 270–290 nm in the CD signal curve according with the B-DNA structure. However, when adding OFL into the solution, the trend of the CD signal curve has been changed. At 2 μM OFL, the negative peak declines mildly and the positive peak in the wavelength from 270–290 nm reaches to approximately 0.0 mdeg, which shows that the base stacking of DNA has been changed based on n/π* and π-π* transitions and hydrogen bond. Therefore, it can be concluded that the aptamer is combined with OFL in the solution and verify the principle.

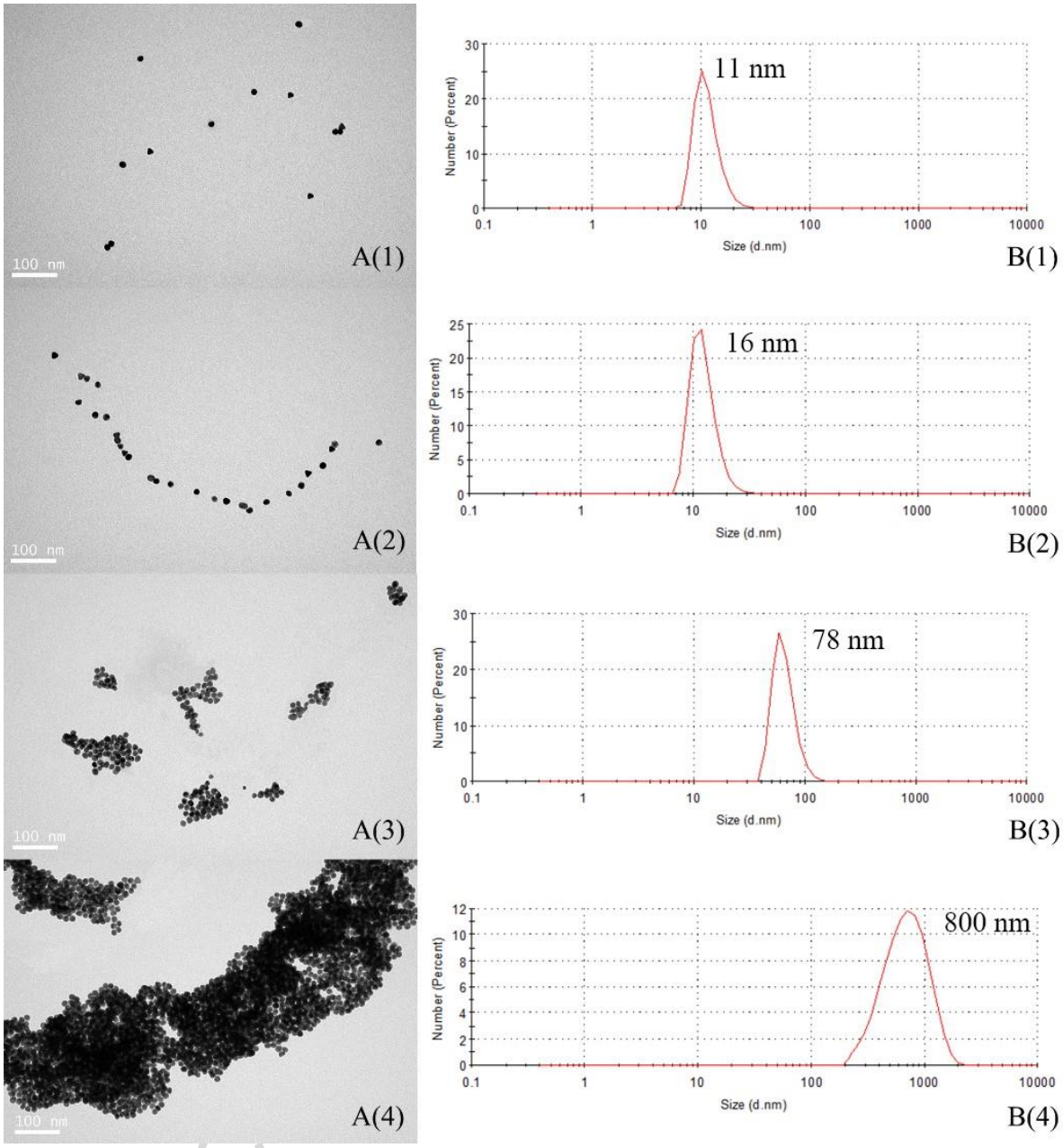

Fig. 2 Different transmission electron microscope (TEM) images (A) and dynamic light scattering (DLS) images (B) of the AuNPs solutions in different substances: (a) AuNPs; (b) AuNPs + 10 nM aptamer +120 mM NaCl; (c)AuNPs + 10 nM aptamer + 120 mM NaCl + 500 nM OFL; (d)AuNPs + 10 nM aptamer + 120 mM NaCl + 1000 nM OFL. The volume of each sample in TEM and DLS is 500 μL and 5 mL, respectively.

To further prove the sensing principle of this biosensor, TEM and DLS were employed to characterize the different sizes of AuNPs in dispersion–aggregation behavior in the solution caused by the concentration of NaCl. As shown in Fig. 2, the particle morphology and the size distribution curve of AuNPs in TEM and DLS were obtained in graphs (A) and graphs (B), respectively. The bare AuNPs show great spherical shape and extremely dispersion (Fig. 2 A, 1), and the average diameter of the original AuNPs is 11 nm (Fig. 2 B, 1). After the addition of the aptamers into the solution, AuNPs are protected due to coated with aptamers. Thus, the addition of

the NaCl could not make the AuNPs aggregated (Fig. 2 A, 2), and the average diameter of AuNPs becomes slightly larger as 16 nm (Fig. 2 B, 2) due to insufficient reaction time and the interaction between AuNPs–aptamers and AuNPs. After the addition of OFL, since the interaction between aptamers and OFL is stronger than the interaction between AuNPs and aptamers, the aptamers–OFL compound is formed and the bare AuNPs are released to the solution. Under the influence of NaCl, AuNPs become aggregated into obvious clusters (Fig. 2 A, 3). Hence, the average diameter of AuNPs becomes larger to 78 nm gradually at 300 nM OFL (Fig. 2 B, 3). With the increasing concentration of OFL, AuNPs gather into a cluster (Fig. 2 A, 4), and the average diameter of AuNPs is 800 nm ultimately at 1500 nM OFL (Fig .2 B, 4). According to the average diameter changes of AuNPs in different situations, the principle of the biosensor for detecting OFL is viable.

3.3 Optimization of detecting conditions

This sensing system is based on the optimized concentrations of NaCl, aptamer, RB for completed reaction. Appropriate incubating temperature and pH of the MOPS buffer are significant to maintain the properties of the aptasensor. Thus, following optimization were performed, (Fig. S1) the concentration of NaCl, (Fig. S2) the concentration of OFL specific aptamer, (Fig. S3) the incubating temperature of the system, and (Fig. S4) pH of MOPS buffer, (Fig. S5) the concentration of Rhodamine B. Fig. S1 shows that the trend of A650/A520 is influenced by the concentration of NaCl, and the maximum of A650/A520 is reached when the concentration of NaCl is greater than or equal to 120 mM. So the optimized concentration of NaCl is 120 mM, which can make AuNPs fully aggregated and save the materials. Fig. S2 reveals that specific OFL aptamer plays two roles in the reaction: forming compounds with OFL and preventing AuNPs from aggregated. The aptamer concentration of 10 nM in the solution brings the situation into a balance and achieves the maximum of ΔA650/A520, which is the optimal concentration of the aptamer in the system. In Fig. S3 and Fig. S4, the trend of curves clearly suggests that an increasing number of aptamers bind to OFL in the initial part because ascending temperature and pH activate the particles in the solution [37]. When temperature and pH go beyond the optimal value, the property of elements in the reaction will be damaged, and the amount of aggregated AuNPs will markedly decrease. Fig. S3 shows that the temperature of 28 ℃ is the optimal incubating temperature and Fig. S4 shows that the optimal pH of the MOPS buffer for the best stability and complexity of the reaction is 7. Fig. S5 suggests that 9 nM of the concentration of Rhodamine B in this system achieves the most obvious difference in fluorescence intensity with or without OFL, and 9 nM of RB can maximize the fluorescence signal converted from colorimetric signal.

3.4 Sensitivity for OFL detection of the system

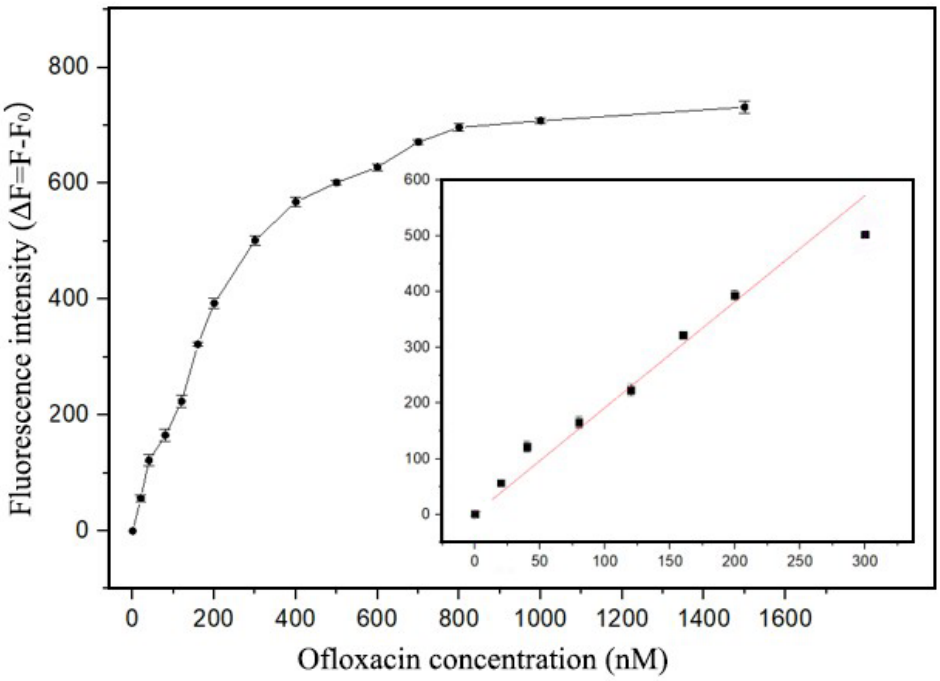

Fig. 3 Sensitivity of the sensing system with 0, 20, 40, 80, 120, 160, 200, 300, 400, 500, 600, 700, 800, 1000 and 1500 nM OFL. F represents fluorescence intensity tested with OFL and F_0 represents fluorescence intensity of blank system. Inset: linear fitting curve of the sensing system for OFL in range of 20-300 nM. Sensing system: 28 °C, 100 μL AuNPs, 120 mM NaCl, 10 nM aptamer, 9 μM RB, 3-(N-Morpholino) propanesulfonic acid (MOPS) buffer (10 mM, pH 7.0).

For the sensivitity of the system, ΔF in different concentrations of OFL was measured under the optimal conditions. As shown in Fig. 3, the working curve is linearly growing till 300 nM. With the increasing concentration of OFL, the growth of ΔF gradually slowdowns, and ultimately ΔF is invariant. In the range of low concentration of OFL (20 nM–300 nM) , the relation between ΔF and OFL concentration has a linear curve with a equation of $\Delta F = 1.6954c_{OFL} + 38.1309$ (R=0.9907). Based on the previous studies [37], 3σ/slope is used to determine the limit of detection (LOD). The standard deviation (σ) of the instrument was calculated from the results of 8 repetitions of blank sample containing 400 μL of MOPS buffer and 100 μL of AuNPs. Thus, the LOD is calculated as 1.66 nM.

Compared with the reported methods of detecting OFL shown in Table 1, this fluorescent aptasensor has merits and demerits. The LOD is lower than several methods except some advanced electrochemical sensors [17, 27] and the modified fluorescence sensor [38]. Nevertheless, this method does not need precision instruments, fluorescent labelling and complex modifications of the aptamer . The method has the practicability for the detection of OFL in the environment and food, because of the moderate sensitivity, low requirement of instruments and the simple process.

Table 1

Comparison with other reported methods for the detection of OFL

Method	Linear range (nM)	LOD (nM)	Application	Reference
Automated HPLC–FLD	2-500	2	Chicken meat	[13]
HPLC with fluorescence detection	28-2.8×10^5	28	Aqueous vitreous	[14]
Electrochemical sensor based on NG	500-2.75×10^4	340	Clinical samples	[15]
Electrochemical sensor based on Pt-Au	80-1×10^4 1×10^4-1×10^5	50	Urine Tablet	[13]
Electrochemical aptasensor	50-2000	1	Effluent of sewage treatment plant	[27]
Electrochemical sensor based on GO and ionic liquid	7-700	0.28	Urine ophthalmic	[17]
Capillary electrophoresis	Not mentioned	9	Urine	[39]
Colorimetric aptasensor	2.0-400	3.38	Tap water	[28]
Spectrofluorimetry with magnetic nanoparticles	140-1269	33.6	Plasma urine	[40]
Fluorescence based on silver nanoclusters-Cu^{2+}	0.1-80	0.049	Urine tablet	[38]
Fluorometry based on AuNPs quenching RB	20-300	1.66	Milk	Present work

HPLC: High Performance Liquid Chromatography, FLD: fluorescence detector, NG: nitrogen-doped graphene nanocomposites, GO: graphene oxide.

3.5 Selectivity for OFL detection of the system

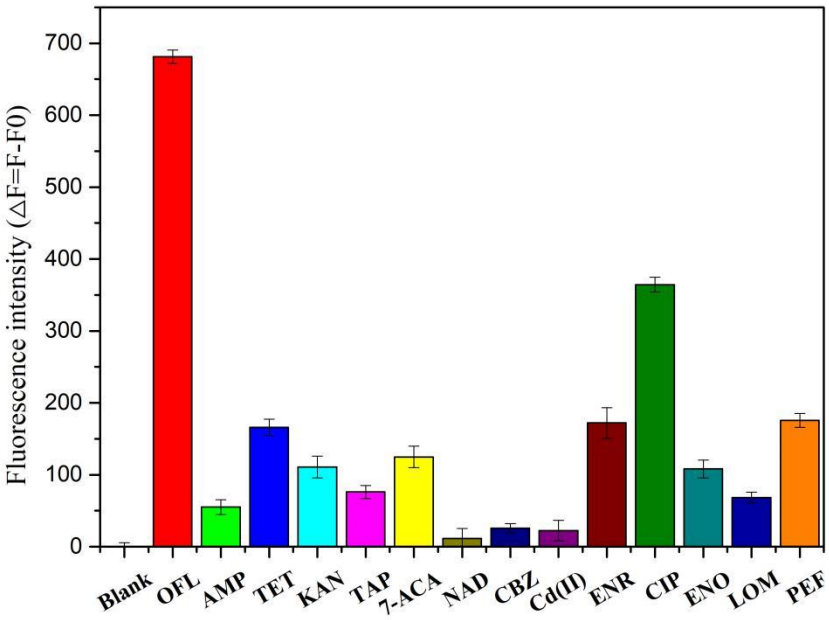

Fig. 4 Selectivity of the method for OFL detection. Reagents: ofloxacin (OFL), ampicillin (AMP), tetracycline (TET), kanamycin (KAN), thiamphenicol (TAP), 7– aminocephalosporanic acid (7–ACA), Nalidixic acid (NAD) and carbendazim (CBZ), Cd^{2+}, enrofloxacin (ENR), ciprofloxacin (CIP), enoxacin (ENO), lomefloxacin (LOM) and pefloxacin (PEF) of 1 μM; Sensing system: 28 °C, 100 μL AuNPs, 120 mM NaCl, 10 nM aptamer, 9 μM RB, 3-(N-Morpholino) propanesulfonic acid (MOPS) buffer (10 mM, pH 7.0).

For the selectivity of the assay, OFL and some interferents such as other structural analogues(NAD,ENR,CIP, LOM, PEF), quinolone antibiotics (ENO), common antibiotics (AMP, TET, KAN, TAP, 7-ACA), pesticide (CBZ) and metal ions (Cd^{2+}) were tested under the optimized conditions. Fig. 4 shows that OFL causes very obvious fluorescent signal than other interferents except CIP.

As for ciprofloxacin (CIP), since the target originally selected for this aptamer is ofloxacin and its structurally similar fourth-generation quinolone antibiotics, including ciprofloxacin [26]. Additionally, the structures and functional groups of ofloxacin and ciprofloxacin are similar. Hence, it is reasonable that the aptamer has a relatively obvious fluorescent signal to ciprofloxacin, but there is still a significant difference between it and ofloxacin.

In conclusion,, Fig. 4 could demonstrate that this method has good selectivity for OFL detection.

3.6 Applications in milk samples

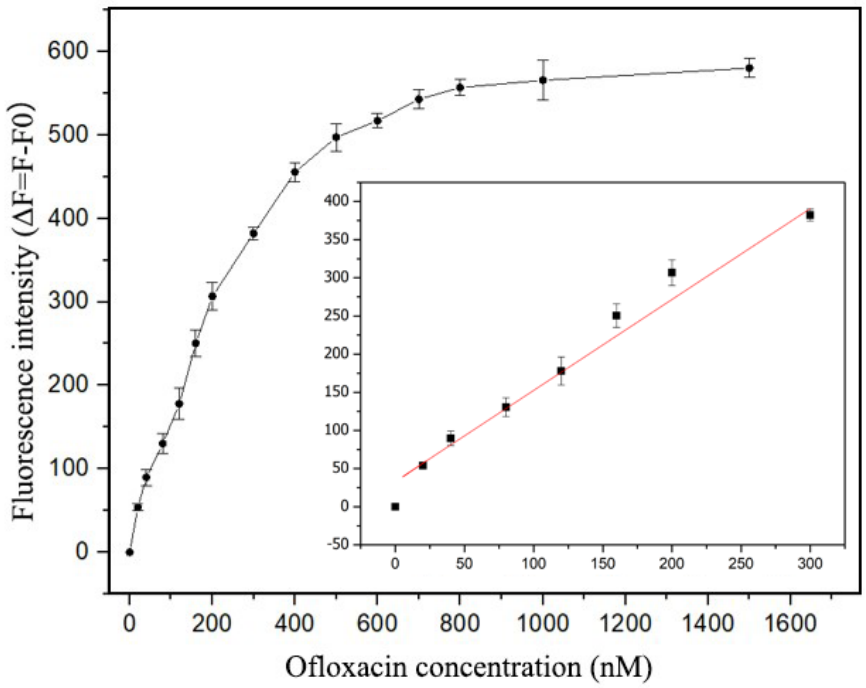

Fig. 5 Sensitivity of the sensing system in milk samples added 0, 20, 40, 80, 120, 160, 200, 300, 400, 500, 600, 700, 800, 1000 and 1500 nM OFL. Inset: linear fitting curve of the sensing system for OFL in range of 20-300 nM. Sensing system: 28°C, 100 μL AuNPs, 120 mM NaCl, 10 nM aptamer, 9 μM RB, 3-(N-Morpholino) propanesulfonic acid (MOPS) buffer (10 mM, pH 7.0).

To achieve relatively reliable precision for detecting OFL in milk samples, a referential working curve and the LOD in milk samples were performed. By the process similar to the former sensitivity test, 0, 20, 40, 80, 120, 160, 200, 300, 400, 500, 600, 700, 800, 1000, 1500 nM of OFL dissolved in milk samples, 100 μL AuNPs, 120 mM NaCl, 10 nM aptamer and 9 nM Rhodamine B were added to build the working curve in milk samples, which further proved the practicability for the actual detection. As shown in Fig. 5, the whole series of ΔF were smaller than that in MOPS buffer, while the trend of curve was similar to the former result. In the linear range from 20 to 300 nM, the fitted equation is $\Delta F=1.19157c_{OFL}+33.26628$ ($R=0.9963$). As mentioned, the LOD was calculated as 4.61 nM (1.66 μg/L).

The recovery and the relative standard deviation (RSD) were tested by added different concentrations of OFL (0, 50, 100, 150, 200 nM) into milk samples. The ΔF was plugged into the linear equation to calculate the recovery, and RSD was calculated by difference between three parallel tests. As shown in Table 2, the recoveries and RSD were kept within 86.97% to 103.81% and 3.13% to 9.59%.

Table 2

Determination of OFL in milk samples

Spiked OFL (nM)	Found concentration (nM)			Mean Found (nM)	Recovery (%)	RSD (%)
	1	2	3			
50	45.98	44.79	39.69	43.48	86.97	3.13
100	82.37	103.79	84.57	90.24	90.24	9.59
150	152.38	143.46	164.12	153.32	102.23	5.59
200	198.25	216.25	208.34	207.61	103.81	3.57

RSD (relative standard deviation) = SD (standard deviation) / mean found

Compared with the other methods of detecting OFL in milk samples shown in Table 3, although the RSD of this assay are slightly higher, but it has moderate LOD and no need of sophisticated extraction, or complicated process in derivative methods of HPLC. In addition, the LOD of OFL is clearly lower than the maximum residue level (MRL) set by the European Union (≈30 μg/L) [41]. The convenience and low–cost of the assay make it possible to be applied in practical milk test, but the matter of simplifying pretreatments for milk cannot be ignored. Thus, there is still a demand for the quick detection of dairy products in the actual conditions. Moreover, good results of the application in strong-interference system such as the milk samples show the feasibility of applications in other food samples.

Table 3

Comparison with other reported methods of the detection of OFL in milk

Method	RSD (%)	LOD (nM)	Reference
MIMSPE	1.9 - 9.2	3.2 μg/kg	[42]
HPLC-FLD	3.4	0.466 μg/kg	[43]
HPLC-MS	3.9	0.6 μg/kg	[44]
Fluorescence spectrophotometry	4.7 - 11.8	10 μg/kg	[45]
Aluminium sensitized spectrofluorimetry	0.83 - 1.87	16 μg/kg	[46]
Fluorometry based on AuNPs quenching	3.13 - 9.59	1.66 μg/kg	Present work

MIMSPE: magnetic solid phase extraction, HPLC: High Performance Liquid Chromatography, FLD: fluorescence detector, MS: mass spectrometry.

4. Conclusions

A new fluorescent aptasensor for OFL detection based on decreased fluorescence caused by AuNPs quenching Rhodamine B has been established. The fluorescent intensity of RB is affected by the aggregation degree of AuNPs, which is regulated by certain concentration of OFL. This method can specifically, sensitively measure OFL by simple process, cheap instruments and short

time. The limit of detection in MOPS buffer is 1.66 nM with linear range from 20 to 300 nM. Besides, the limit of detection in milk samples is 4.61 nM with recovery from 86.97% to 103.81% and RSD from 3.13% to 9.59%, which indicates the availability of this aptasensor for further practical detection in milk or dairy samples.

5. Acknowledgements

This work was sponsored by the National Key Research and Development Program of China (2017YFD0800704), and the Natural Science Foundation of Zhejiang Province (LY18B070029).

6. Compliance with ethical standards

The author(s) declare that they have no competing interests.

7. References

[1] K. Mitani, H. Kataoka, Determination of fluoroquinolones in environmental waters by in-tube solid-phase microextraction coupled with liquid chromatography-tandem mass spectrometry, Anal Chim Acta, 562 (2006) 16-22.

[2] O. Ballesteros, J.L. Vilchez, A. Navalon, Determination of the antibacterial ofloxacin in human urine and serum samples by solid-phase spectrofluorimetry, J Pharmaceut Biomed, 30 (2002) 1103-1110.

[3] D. Sood, N. Kumar, A. Singh, M.K. Sakharkar, V. Tomar, R. Chandra, Antibacterial and Pharmacological Evaluation of Fluoroquinolones: A Chemoinformatics Approach, Genomics & Informatics, 16 (2018) 44-51.

[4] F.U. Khan, F. Nasir, Z. Iqbal, I. Khan, N. Shahbaz, M. Hassan, F. Ullah, Simultaneous determination of moxifloxacin and ofloxacin in physiological fluids using high performance liquid chromatography with ultraviolet detection, J Chromatogr B, 1017 (2016) 120-128.

[5] C. Vakh, M. Alaboud, S. Lebedinets, A. Bulatov, A rotating cotton-based disk packed with a cation-exchange resin: Separation of ofloxacin from biological fluids followed by chemiluminescence determination, Talanta, 196 (2019) 117-123.

[6] B.R. Esposito, M.L. Capobianco, A. Martelli, M.L. Navacchia, L. Pretali, M. Saracino, A. Zanelli, S.S. Emmi, Advanced water remediation from ofloxacin by ionizing radiation, Radiat Phys Chem, 141 (2017) 118-124.

[7] H. Mu, Z. Xu, Y. Liu, Y. Sun, B. Wang, X. Sun, Z. Wang, S. Eremin, A.V. Zherdev, B.B. Dzantiev, H. Lei, Probing the stereoselective interaction of ofloxacin enantiomers with corresponding monoclonal antibodies by multiple spectrometry, Spectrochim Acta A, 194 (2018) 83-91.

[8] S. Adhikari, D. Kim, Synthesis of Bi2S3/Bi2WO6 hierarchical microstructures for enhanced visible light driven photocatalytic degradation and photoelectrochemical sensing of ofloxacin, Chem Eng J, 354 (2018) 692-705.

[9] S. Liu, G. Dong, H. Zhao, M. Chen, W. Quan, B. Qu, Occurrence and risk assessment of fluoroquinolones and tetracyclines in cultured fish from a coastal region of northern China, Environ Sci Pollut R, 25 (2018) 8035-8043.

[10] A.A. Alhusban, O.A. Tarawneh, S.O. Dawabsheh, A.A. Alhusban, F.W. Abumhareb, Liquid chromatography-tandem mass spectrometry for rapid and selective simultaneous determination of

fluoroquinolones level in human aqueous humor., J Pharmacol Tox Met, 97 (2019) 36-43.
[11] S.A. Muthu, N. Mothi, S.M. Shiriskar, R.R.S. Pissurlenkar, A. Kumar, B. Ahmad, Physical basis for the ofloxacin-induced acceleration of lysozyme aggregation and polymorphism in amyloid fibrils, Arch Biochem BiophyS, 592 (2016) 10-19.
[12] C. Chafer-Pericas, A. Maquieira, R. Puchades, J. Miralles, A. Moreno, Multiresidue determination of antibiotics in feed and fish samples for food safety evaluation. Comparison of immunoassay vs LC-MS-MS, Food Control, 22 (2011) 993-999.
[13] I. Timofeeva, S. Timofeev, L. Moskvin, A. Bulatov, A dispersive liquid-liquid microextraction using a switchable polarity dispersive solvent. Automated HPLC-FLD determination of ofloxacin in chicken meat, Anal Chim Acta, 949 (2017) 35-42.
[14] K.P. Chan, K.O. Chu, W.W. Lai, K.W. Choy, C.C. Wang, D.S. Lam, C.P. Pang, Determination of ofloxacin and moxifloxacin and their penetration in human aqueous and vitreous humor by using high-performance liquid chromatography fluorescence detection, Anal Biochem, 353 (2006) 30-36.
[15] F. Wu, F. Xu, L. Chen, B. Jiang, W. Sun, X. Wei, Cuprous Oxide/Nitrogen-doped Graphene Nanocomposites as Electrochemical Sensors for Ofloxacin Determination, Chem Res Chinese U, 32 (2016) 468-473.
[16] Z. Jiang, Q. Liu, Y. Tang, M. Zhang, Electrochemical Sensor Based on a Novel Pt-Au Bimetallic Nanoclusters Decorated on Reduced Graphene Oxide for Sensitive Detection of Ofloxacin, Electroanal, 29 (2017) 602-608.
[17] A. Wong, T.A. Silva, F.C. Vicentini, O. Fatibello-Filho, Electrochemical sensor based on graphene oxide and ionic liquid for ofloxacin determination at nanomolar levels, Talanta, 161 (2016) 333-341.
[18] C. Vakh, A. Pochivalov, S. Koronkiewicz, S. Kalinowski, V. Postnov, A. Bulatov, A chemiluminescence method for screening of fluoroquinolones in milk samples based on a multi-pumping flow system, Food Chem, 270 (2019) 10-16.
[19] C.S.P. Sastry, K.R. Rao, D.S. Prasad, Extractive spectrophotometric determination of some fluoroquinolone derivatives in pure and dosage forms, Talanta, 42 (1995) 311-316.
[20] A.P. Pagani, G.A. Ibanez, Analytical approach for the simultaneous determination of quinolones in edible animal products. Modeling pH-modulated fluorescence excitation-emission matrices four-way arrays, Talanta, 192 (2019) 52-60.
[21] X. Wang, Y. Li, R. Li, H. Yang, B. Zhou, X. Wang, Y. Xie, Comparison of chlorination behaviors between norfloxacin and ofloxacin: Reaction kinetics, oxidation products and reaction pathways, Chemosphere, 215 (2019) 124-132.
[22] A.D. Ellington, J.W. Szostak, In vitro selection of RNA molecules that bind specific ligands, Nature, 346 (1990) 818-822.
[23] C. Tuerk, L. Gold, Systematic evolution of ligands by exponential enrichment: RNA ligands to bacteriophage T4 DNA polymerase, Science, 249 (1990) 505.
[24] L. Wang, C. Wang, H. Li, Selection of DNA aptamers and establishment of an effective aptasensor for highly sensitive detection of cefquinome residues in milk, Analyst, 143 (2018) 3202-3208.
[25] J. Zhang, B. Zhang, Y. Wu, S. Jia, T. Fan, Z. Zhang, C. Zhang, Fast determination of the tetracyclines in milk samples by the aptamer biosensor, Analyst, 135 (2010) 2706-2710.
[26] C. Reinemann, U.F. von Fritsch, S. Rudolph, B. Strehlitz, Generation and characterization of quinolone-specific DNA aptamers suitable for water monitoring, Biosens Bioelectron, 77 (2016) 1039-1047.
[27] S. Pilehvar, C. Reinemann, F. Bottari, E. Vanderleyden, S. Van Vlierberghe, R. Blust, B. Strehlitz, K.

De Wael, A joint action of aptamers and gold nanoparticles chemically trapped on a glassy carbon support for the electrochemical sensing of ofloxacin, Sensor Actuat B-Chem, 240 (2017) 1024-1035.
[28] X. Zhou, L. Wang, G. Shen, D. Zhang, J. Xie, A. Mamut, W. Huang, S. Zhou, Colorimetric determination of ofloxacin using unmodified aptamers and the aggregation of gold nanoparticles, Microchim Acta, 185 (2018).
[29] S. Zhan, Y. Wu, L. He, F. Wang, X. Zhan, P. Zhou, S. Qiu, A silver-specific DNA-based bio-assay for Ag(I) detection via the aggregation of unmodified gold nanoparticles in aqueous solution coupled with resonance Rayleigh scattering, Anal Methods-Uk, 4 (2012) 3997-4002.
[30] E. Priyadarshini, N. Pradhan, Gold nanoparticles as efficient sensors in colorimetric detection of toxic metal ions: A review, Sensor Actuat B-Chem, 238 (2017) 888-902.
[31] Y. Luo, L. He, S. Zhan, Y. Wu, L. Liu, W. Zhi, P. Zhou, Ultrasensitive Resonance Scattering (RS) Spectral Detection for Trace Tetracycline in Milk Using Aptamer-Coated Nanogold (ACNG) as a Catalyst, J Agr Food Chem, 62 (2014) 1032-1037.
[32] J. Xu, Y. Li, L. Wang, Y. Huang, D. Liu, R. Sun, J. Luo, C. Sun, A facile aptamer-based sensing strategy for dopamine through the fluorescence resonance energy transfer between rhodamine B and gold nanoparticles, Dyes Pigments, 123 (2015) 55-63.
[33] H. Zhang, L. Wang, W. Jiang, Label free DNA detection based on gold nanoparticles quenching fluorescence of Rhodamine B, Talanta, 85 (2011) 725-729.
[34] S. Zhan, H. Xu, X. Zhan, Y. Wu, L. Wang, J. Lv, P. Zhou, Determination of silver(I) ion based on the aggregation of gold nanoparticles caused by silver-specific DNA, and its effect on the fluorescence of Rhodamine B, Microchim Acta, 182 (2015) 1411-1419.
[35] N. Duan, S. Wu, S. Dai, H. Gu, L. Hao, H. Ye, Z. Wang, Advances in aptasensors for the detection of food contaminants, Analyst, 141 (2016) 3942-3961.
[36] K.C. Grabar, R.G. Freeman, M.B. Hommer, M.J. Natan, Preparation and Characterization of Au Colloid Monolayers, Anal Chem, 67 (1995) 735-743.
[37] S. Zhan, Y. Wu, L. Liu, H. Xing, L. He, X. Zhan, Y. Luo, P. Zhou, A simple fluorescent assay for lead(II) detection based on lead(II)-stabilized G-quadruplex formation, Rsc Adv, 3 (2013) 16962-16966.
[38] B. Mao, F. Qu, S. Zhu, J. You, Fluorescence turn-on strategy based on silver nanoclusters-Cu2+ system for trace detection of quinolones, Sensors And Actuators B: Chemical, 234 (2016) 338-344.
[39] H. Sun, P. He, Y. Lv, S. Liang, Effective separation and simultaneous determination of seven fluoroquinolones by capillary electrophoresis with diode-array detector, J Chromatogr B, 852 (2007) 145-151.
[40] M. Amoli-Diva, K. Pourghazi, S. Hajjaran, Dispersive micro-solid phase extraction using magnetic nanoparticle modified multi-walled carbon nanotubes coupled with surfactant-enhanced spectrofluorimetry for sensitive determination of lomefloxacin and ofloxacin from biological samples, Mat Sci Eng C-Mater, 60 (2016) 30-36.
[41] H. Zheng, J. Mo, Y. Zhang, Q. Gao, J. Ding, Q. Yu, Y. Feng, Facile synthesis of magnetic molecularly imprinted polymers and its application in magnetic solid phase extraction for fluoroquinolones in milk samples, J Chromatogr A, 1329 (2014) 17-23.
[42] E.U. Council Regulation and (EEC) No. 2377, 90. n. Official Journal of European Communities, 224 (1990) 1–8.
[43] M. Gao, H. Wang, M. Ma, Y. Zhang, X. Yin, R.A. Dahlgren, D. Du, X. Wang, Optimization of a phase separation based magnetic-stirring salt-induced liquid-liquid microextraction method for determination of fluoroquinolones in food, Food Chem, 175 (2015) 181-188.

[44] A. Junza, N. Dorival-García, A. Zafra-Gómez, D. Barrón, O. Ballesteros, J. Barbosa, A. Navalón, Multiclass method for the determination of quinolones and β-lactams, in raw cow milk using dispersive liquid–liquid microextraction and ultra high performance liquid chromatography–tandem mass spectrometry, J Chromatogr A, 1356 (2014) 10-22.
[45] T. Zhao, B. Yu, W. Tang, H. Zhang, Spectrofluorimetric determination of ofloxacin in milk with N-(9-fluorenylmethyloxycarbonyl)-L-alanine, Spectrochim Acta A, 148 (2015) 125-130.
[46] Q. Xia, Y. Yang, M. Liu, Aluminium sensitized spectrofluorimetric determination of fluoroquinolones in milk samples coupled with salting-out assisted liquid-liquid ultrasonic extraction, Spectrochim Acta A, 96 (2012) 358-364.

Graphical Abstract

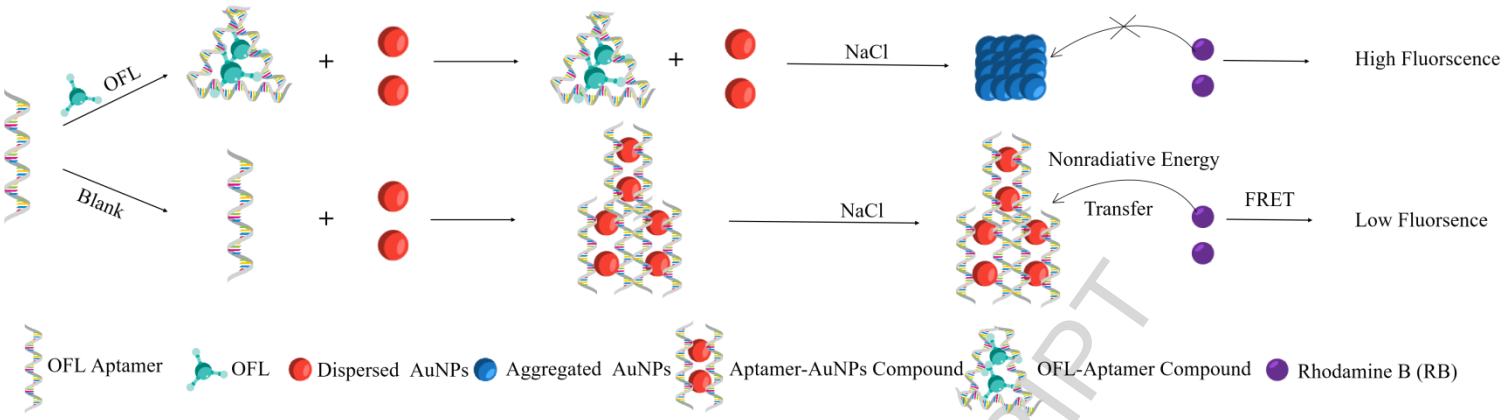

A sensitive and simple fluorescent aptasensor was developed for ofloxacin (OFL) detection in aqueous and milk samples based on the dispersed gold nanoparticles to quenching fluorescence of Rhodamine B.

Highlights

- This method has strong specificity to target and can effectively avoid interference of other substances in the analysis samples.
- LOD of this method is low in both of aqueous and milk samples, as well as the detection range are wild.
- Compared with other traditional methods, it has the advantages of low cost, simple operation and obvious results.
- The recovery was ideal and the results were reproducible

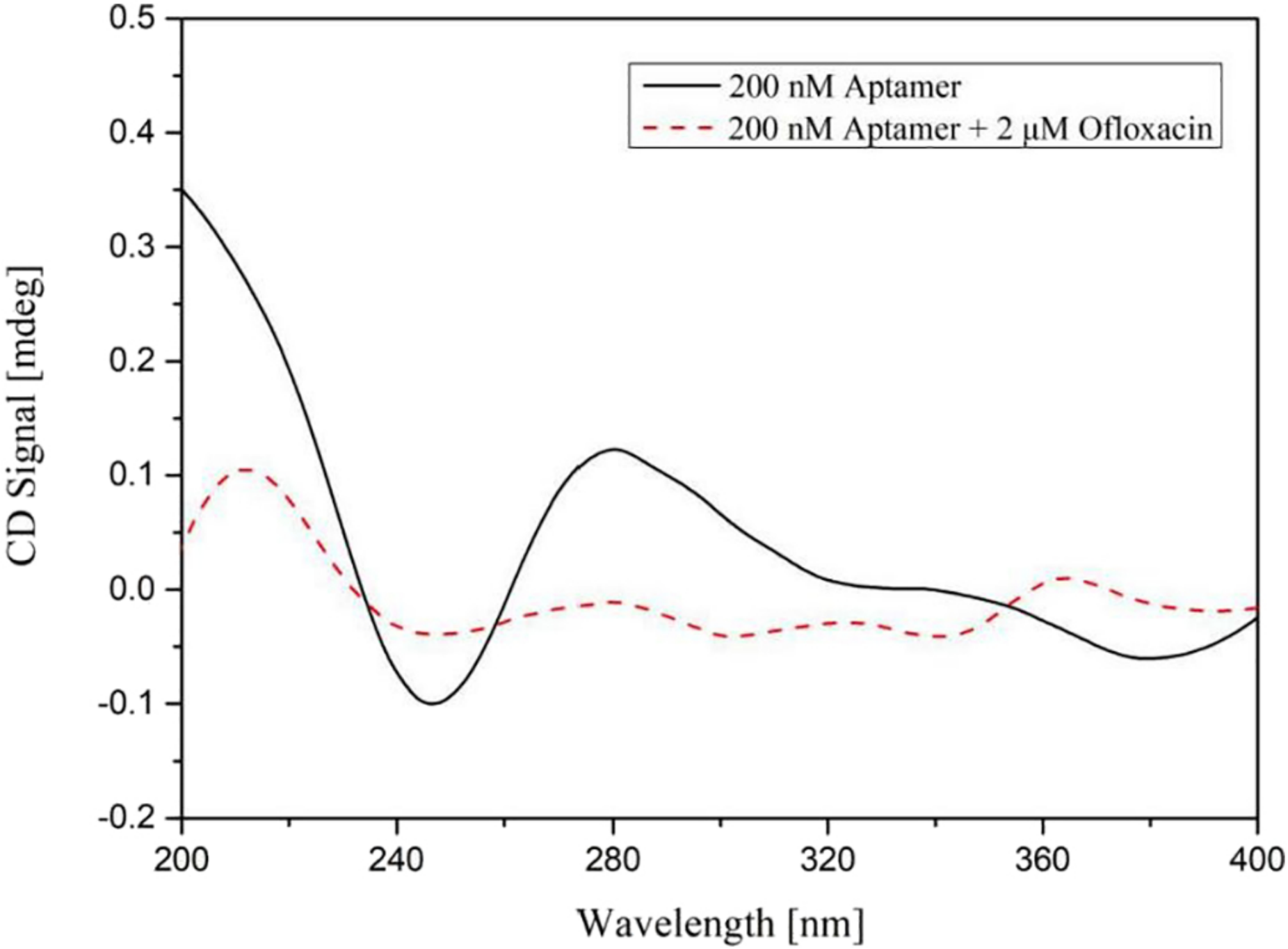
0.5
0.4
0.3
0.2
0.1
0.0
-0.1
-0.2
CD Signal [mdeg]
200
240
280
320
360
400
Wavelength [nm]
200 nM Aptamer
200 nM Aptamer + 2 μM Ofloxacin

Figure 1

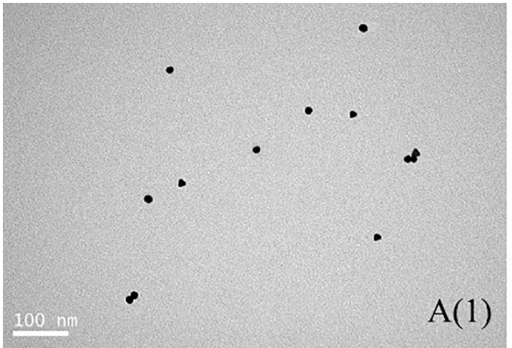
100 nm
A(1)

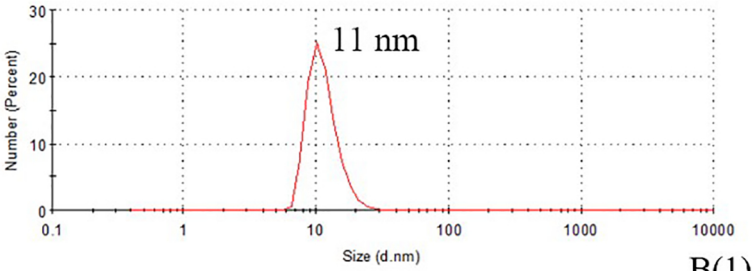
11 nm
Number (Percent)
Size (d.nm)
B(1)

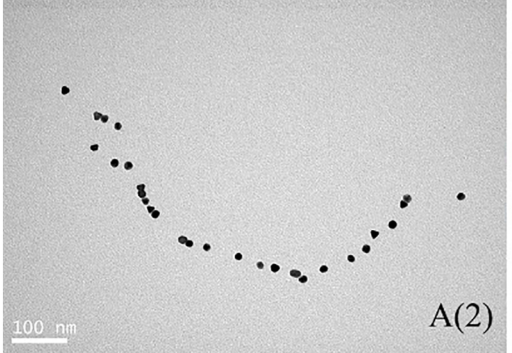
100 nm
A(2)

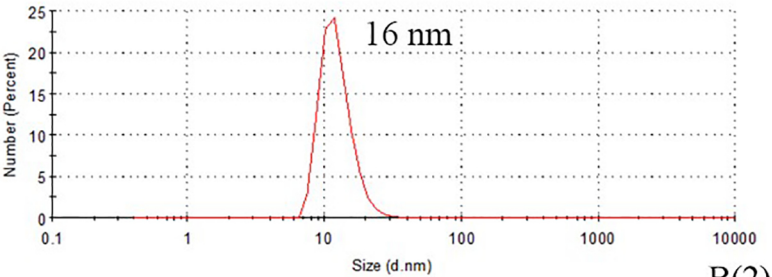
16 nm
Number (Percent)
Size (d.nm)
B(2)

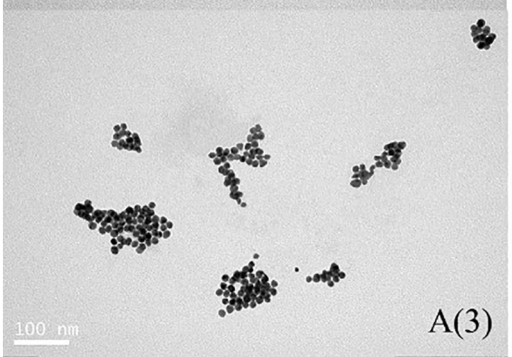
100 nm
A(3)

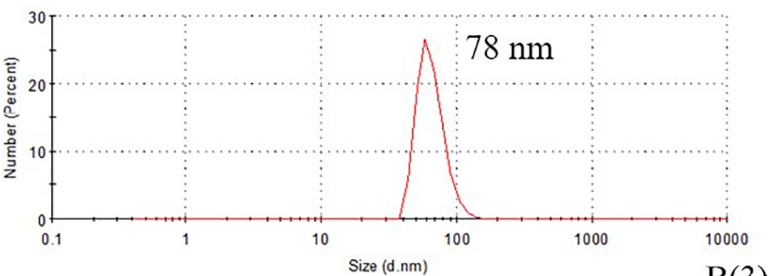
78 nm
Number (Percent)
Size (d.nm)
B(3)

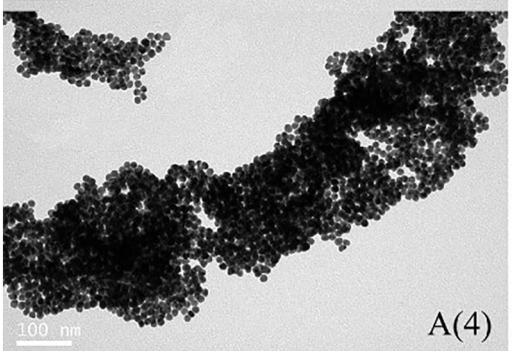
100 nm
A(4)

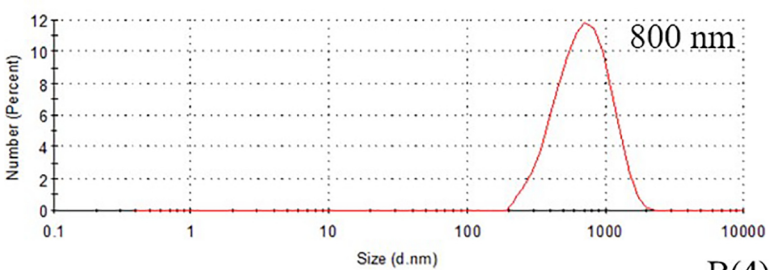
800 nm
Number (Percent)
Size (d.nm)
B(4)

Figure 2

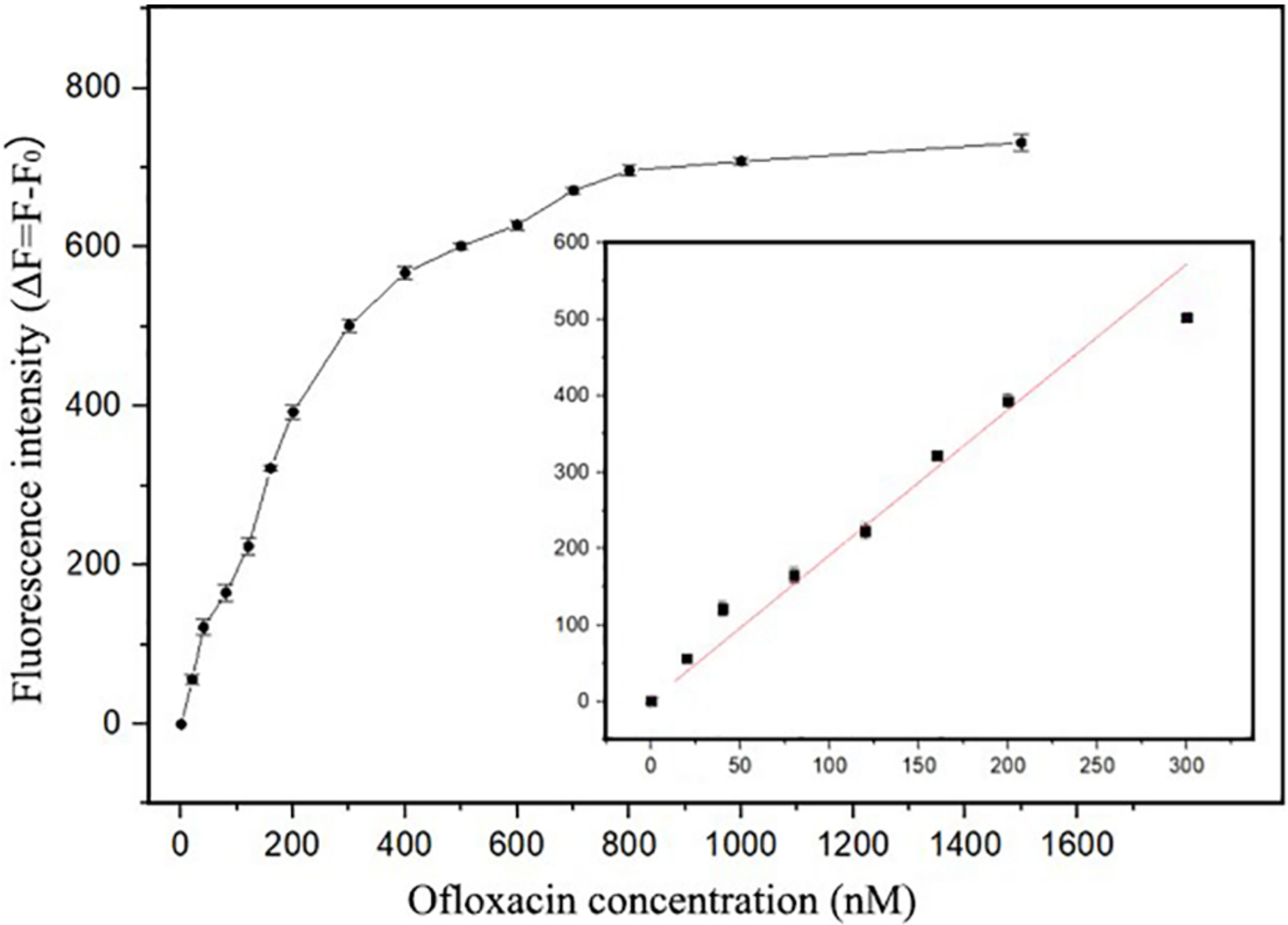
Fluorescence intensity (ΔF=F-F0)
0
200
400
600
800
0
200
400
600
800
1000
1200
1400
1600
Ofloxacin concentration (nM)
0
100
200
300
400
500
600
0
50
100
150
200
250
300

Figure 3

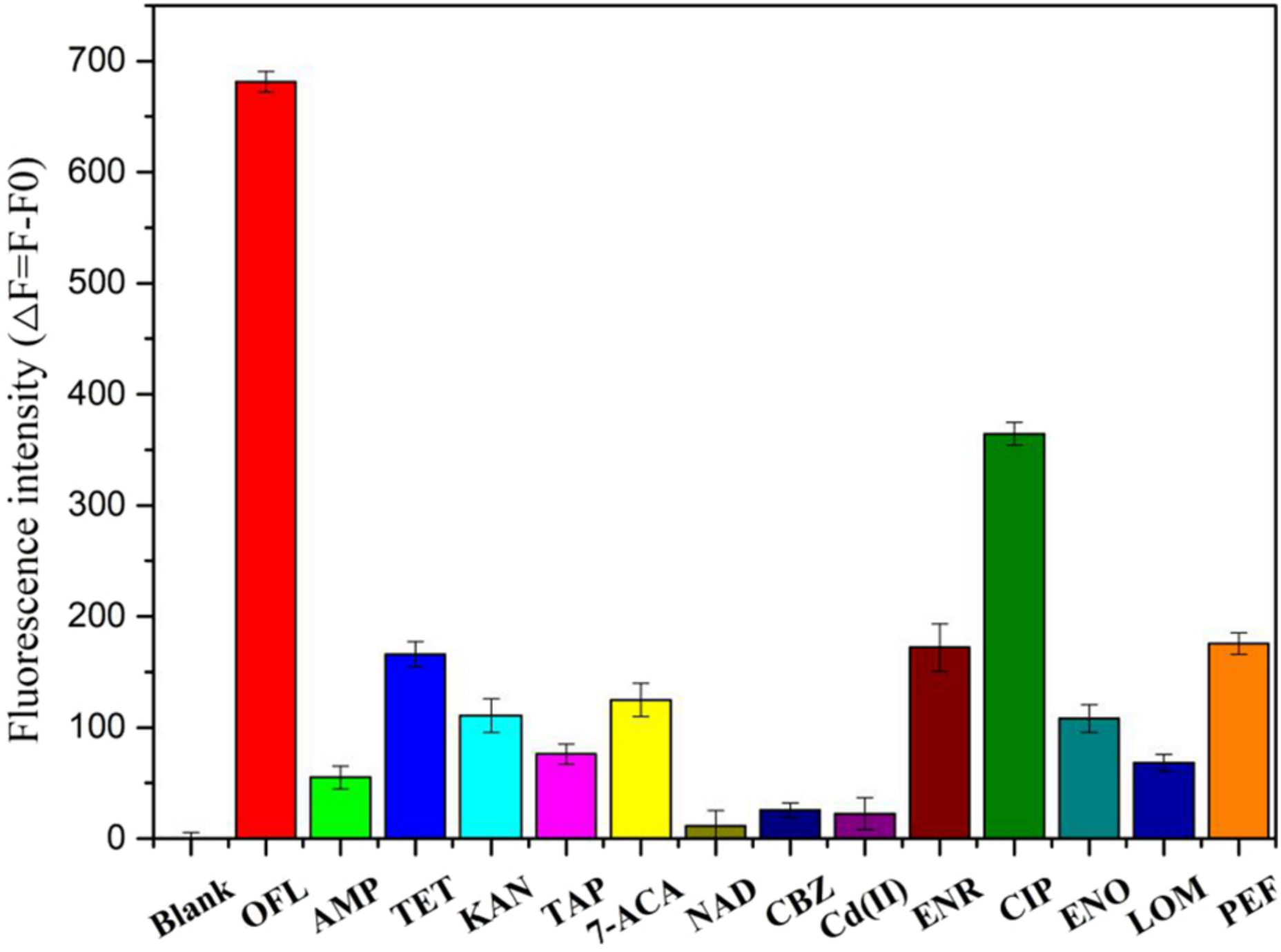
Fluorescence intensity (ΔF=F-F0)
700
600
500
400
300
200
100
0
Blank
OFL
AMP
TET
KAN
TAP
7-ACA
NAD
CBZ
Cd(II)
ENR
CIP
ENO
LOM
PEF

Figure 4

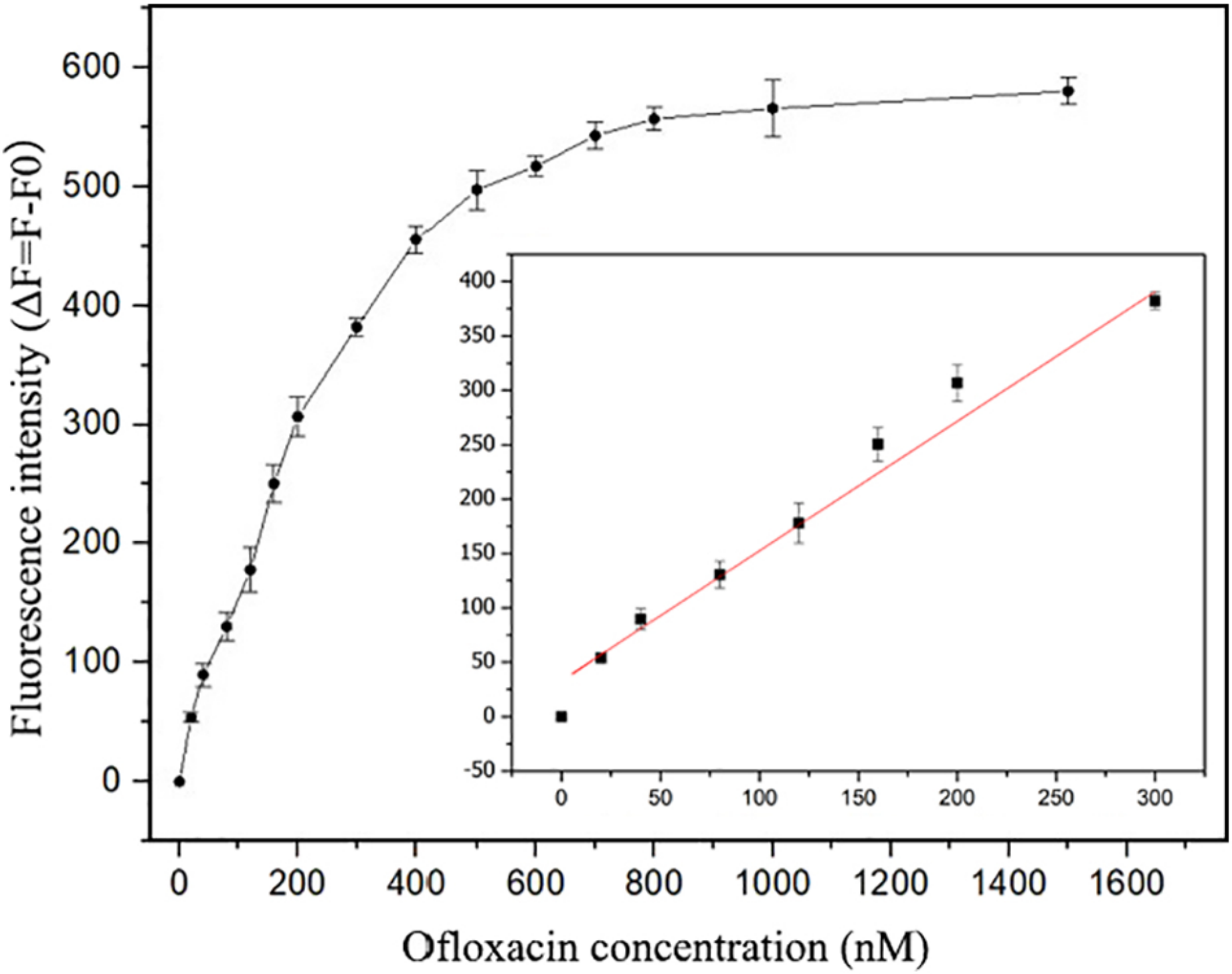
Fluorescence intensity (ΔF=F-F0)
Ofloxacin concentration (nM)
0
100
200
300
400
500
600
0
200
400
600
800
1000
1200
1400
1600
-50
0
50
100
150
200
250
300
350
400

Figure 5